

On the Directional Sea Measurement Using a Circular Array

By
Shigesuke ISHIDA*

SUMMARY

For estimating the directional spectrum of short-crested seas Circular Array Method (CAM) is proposed. CAM is an array-dependent method, distributing wave gauges on a circle and one on the center of the circle. Through this array arrangement the Fourier coefficients of the directional distribution function can be evaluated by a simple calculation, inverse Fourier transformation of cross spectrum. But for higher orders MEM extrapolation is used.

Fourier coefficients are calculated directly and distinctly with simple equation, so it is easier than other methods (e.g. MLM) to estimate the reliability of the result and to find the reason when we get an unexpected directional distribution. For a single-peak distribution the resolution of CAM is satisfactory with a skillful filter, but for complicated distribution there is a room for improvement of MEM extrapolation process.

Standing wave effect caused by a reflection wall can be a serious problem for experiments in model basins and for field measurements. Application of CAM to those wave fields was studied qualitatively and quantitatively. The behavior of the interaction term was discussed relating to the distance of the array from the wall, the array size, the incident angle to the wall and so on. These discussions were confirmed by simulations.

1 INTRODUCTION

Estimating the directional distribution of short-crested seas has been increasingly important for naval architects and civil engineers. Recently some methods based on statistical models have been developed and getting popular like MLM¹⁾, MEM²⁾, MBM³⁾ and so on. These methods are reported to have a better resolution than conventional methods with small number of sensors, but have some instability inherent in the modeling. In this report an array-dependent method, using wave gauges distributed on a circle and on the origin, is proposed. It is basically based on the conventional Fourier series expansion, but supplemented by MEM extrapolation if necessary. Application to the wave fields those are contaminated by reflected waves has also been discussed.

*Ship Dynamics Division

2 PROPERTIES OF CROSS SPECTRUM

In general 3-D wave spectrum $S(f, \theta)$ is expressed as a product of power spectrum $S_0(f)$ and directional distribution function $D(f, \theta)$,

$$S(f, \theta) = S_0(f)D(f, \theta), \quad (1)$$

where $D(f, \theta)$ is normalized like

$$\int_{-\pi}^{\pi} D(f, \theta) d\theta = 1.$$

Cross spectrum of surface elevation measured at two points is

$$\begin{aligned} \Phi(f, \mathbf{r}) &= \int_{-\pi}^{\pi} S(f, \theta) e^{j\mathbf{k}\cdot\mathbf{r}} d\theta \\ &= S_0(f) \int_{-\pi}^{\pi} D(f, \theta) e^{j\mathbf{k}\cdot\mathbf{r}} d\theta \end{aligned} \quad (2)$$

where \mathbf{k} : wave number vector

\mathbf{r} : position vector between two measuring points.

Later frequency f will be dropped for simplicity. Integral signs will mean integrals from $-\pi$ to π . It is a common way to express $D(\theta)$ with a complex Fourier series as follows because it must be a periodic function of 2π ,

$$D(\theta) = \frac{1}{2\pi} \sum_{m=-\infty}^{\infty} \tilde{\rho}_m e^{jm\theta} \quad (3)$$

$$\tilde{\rho}_m = \rho_m e^{j\phi_m} = \tilde{\rho}_{-m}^*, \quad \tilde{\rho}_0 = 1$$

where ρ_m and ϕ_m are the absolute value and the phase of $\tilde{\rho}_m$ respectively. Then cross spectrum which is nondimensionalized by $S_0(f)$ becomes

$$\begin{aligned} \Phi'(\mathbf{r}) &= \int D(\theta) e^{j\mathbf{k}\cdot\mathbf{r}} d\theta \\ &= \sum_{m=-\infty}^{\infty} J_m(kR) \tilde{\rho}_m e^{jm(\alpha + \frac{\pi}{2})} \end{aligned} \quad (4)$$

where $k = |\mathbf{k}|$, $\mathbf{r} = R \begin{pmatrix} \cos\alpha \\ \sin\alpha \end{pmatrix}$.

This equation means that contribution of the component $\tilde{\rho}_m$ to the cross spectrum is proportional to Bessel function $J_m(kR)$. When the argument is small the absolute value of Bessel function rapidly tends to zero with order m . So if kR value is small, i.e. two wave gauges are too close compared to the wave length, it is not easy to evaluate higher order coefficients correctly because in that case cross spectrum includes little information on higher order coefficients, in other words cross spectrum is not sensitive to the detailed shape of $D(\theta)$.

3 CIRCULAR ARRAY METHOD

The idea of Circular Array Method (CAM) is to evaluate $\tilde{\rho}_m$ by inverse Fourier transformation of cross spectrum expressed by eq.(4) with keeping R constant like

$$\tilde{\rho}_m = \frac{1}{J_m(kR)} \frac{1}{2\pi} \int \Phi'(\alpha; R) e^{-jm(\alpha + \frac{\pi}{2})} d\alpha. \quad (5)$$

When we only have N cross spectra with the same spacial distance R and equiangular distribution with the initial angle α_0 like

$$\alpha_n = \alpha_0 + \frac{2\pi}{N}n$$

evaluated coefficient $\hat{\rho}_m$ becomes

$$\begin{aligned} \hat{\rho}_m &= \frac{1}{J_m(kR)} \frac{1}{N} \sum_{n=1}^N \Phi'(\alpha_n; R) e^{-jm(\alpha_n + \frac{\pi}{2})} \\ &= \frac{1}{J_m(kR)} \frac{1}{N} \sum_{n=1}^N \left\{ \sum_{l=-\infty}^{\infty} J_l(kR) \tilde{\rho}_l e^{jl(\alpha_n + \frac{\pi}{2})} \right\} e^{-jm(\alpha_n + \frac{\pi}{2})} \\ &= \sum_{l=-\infty}^{\infty} \frac{J_l(kR)}{J_m(kR)} j^{l-m} f(l-m) \tilde{\rho}_l \end{aligned} \quad (6)$$

where

$$\begin{aligned} f(p) &= \frac{1}{N} \sum_{n=1}^N e^{jp\alpha_n} \\ &= \begin{cases} e^{jp\alpha_0} & p = 0, \pm N, \pm 2N, \dots \\ 0 & \text{other values.} \end{cases} \end{aligned} \quad (7)$$

Substituting eq.(7) to eq.(6) we get

$$\hat{\rho}_m = \sum_{l=-\infty}^{\infty} \frac{J_{m+lN}(kR)}{J_m(kR)} j^{lN} e^{jN\alpha_0} \tilde{\rho}_{m+lN} \quad (8)$$

so, evaluated coefficient $\hat{\rho}_m$ by eq.(6) includes contributions from other Fourier components with the distance of order lN .

We know

$$\begin{aligned}
 \Phi'(-\mathbf{r}) &= \Phi'(\alpha - \pi; R) \\
 &= \Phi'^*(\mathbf{r}) \\
 &= \sum_{m=-\infty}^{\infty} J_m(kR) \tilde{\rho}_m^* e^{-jm(\alpha + \frac{\pi}{2})} \\
 &= \sum_{m=-\infty}^{\infty} (-1)^m J_m(kR) \tilde{\rho}_m e^{jm(\alpha + \frac{\pi}{2})}.
 \end{aligned} \tag{9}$$

Using $\Phi'(\alpha - \pi; R)$ instead of $\Phi'(\alpha; R)$ in eq.(6) and taking an average with eq.(8) we get

$$\hat{\rho}_m = \sum_{l=-\infty}^{\infty} \frac{J_{m+lN}(kR)}{J_m(kR)} j^{lN} e^{jlN\alpha_0} \frac{1 + (-1)^{lN}}{2} \tilde{\rho}_{m+lN}. \tag{10}$$

If N is an odd number we can eliminate contributions from $\hat{\rho}_k$'s, ($k = m \pm N, m \pm 3N, \dots$) like

$$\hat{\rho}_m = \sum_{l=-\infty}^{\infty} \frac{J_{m+2lN}(kR)}{J_m(kR)} (-1)^{lN} e^{2jlN\alpha_0} \tilde{\rho}_{m+2lN}. \tag{11}$$

4 ARRAY DESIGN

We have designed the circular array like Fig.1. N wave gauges (N : odd number) are distributed on the circle and one on the origin. Let us call a group of N gauge pairs those have the same distance R "nest". There are $(N + 1)/2$ nests available.

Nest-0 consists of gauge pairs 0-1, 0-2, 0-3, \dots . For this nest initial angle α_0 is zero and distance R is equal to the radius of the circle A . Nest-1 includes the pairs 1-2, 2-3, 3-4, \dots , nest-2 consists of 1-3, 2-4, 3-5, \dots , and so on. For the nests other than 0 initial angles and distances can be expressed with nest number n_e ,

$$\begin{aligned}
 \alpha_0 &= \frac{\pi}{2} + \frac{\pi}{N} n_e \\
 R &= 2A \sin\left(\frac{\pi}{N} n_e\right).
 \end{aligned}$$

Substituting α_0 to eq.(11) $\hat{\rho}_m$ can be expressed using Kronecker's delta function $\delta(n_e)$

$$\hat{\rho}_m = \sum_{l=-\infty}^{\infty} \frac{J_{m+2lN}(kR)}{J_m(kR)} (-1)^{l\delta(n_e)} \tilde{\rho}_{m+2lN}. \tag{12}$$

We can have $(N + 1)/2$ eqs.(12) for each nests. By solving these simultaneous equations contributions from $(N + 1)/2 - 1$ Fourier components other than order m can be removed.

In principle we can calculate coefficients of any order as long as the number of nests is large enough to remove significant effect from other coefficients in eq.(12). But there is a problem in order $m = 2N$. Using nests other than 0 we can have cross spectra of $2N$ equiangular directions. Directions of gauge pairs of nest-0 are located at the middles of those of other nests. So we can measure cross spectra of $4N$ equiangular directions. All $N(N + 1)/2$ cross spectra measured with this array only have a part of information of wave field which is produced by order $m = \pm 2N$. It is similar to the Nyquist frequency problem in the auto spectrum analysis. So in practice we have to stop calculation at $m = 2N - 1$.

In conventional methods with Fourier series expansion⁴⁾ maximum order is equal to the number of cross spectra using $N(N + 1)/2$ simultaneous equations or is less than that using least-square technique. But evaluated coefficients are not independent with each other, that can lead to an unstable result if some error is included in the cross spectra. Maximum order of CAM is smaller than that but results should be more stable because each coefficients are calculated independently and because we can select nests those include much contribution from the order we are interested in by considering the magnitudes of Bessel functions.

As mentioned before relating to eq.(4), little information of higher order coefficients will be included in the cross spectra if the diameter of the circle is small compared to the wave length we are interested in, that leads to low signal/noise ratio. So the array which has a larger diameter can give more stable and better estimates. The simulation results with statistical noise say the evaluated higher order Fourier coefficients become more stable when the wave length gets shorter. For example if the diameter is close to the wave length we can get a good estimate of the coefficients till about order 10.

Increasing the number of wave gauges not only enables us to go to higher orders but also leads to more stable results because we can select more proper nest(s) which has large $|J_m(kR)|$ value. But considering vulnerability of higher order coefficients to noise and costs, practical number of gauges will be 6, 8 or 10.

5 MEM EXTRAPOLATION

If evaluated maximum order of Fourier coefficients is rather small because of noise or for other reasons $D(\theta)$ will have a serious truncation effect. One solution to avoid that is to extrapolate higher order coefficients using the similar procedure to extrapolating auto correlation function by MEM in the auto spectrum analysis⁵⁾.

If we can assume that Fourier coefficients have the the similar property to auto correlation of wave elevation like

$$\tilde{\rho}_m = E\{f_i f_{i-m}^*\} \quad (13)$$

where $E\{\}$: expected value
 f_i : random Gaussian variable
 $E\{f_i\} = 0$

then we can calculate $\tilde{\rho}_{M+1}$ from $\tilde{\rho}_0, \tilde{\rho}_{\pm 1}, \dots, \tilde{\rho}_{\pm M}$ by

$$\begin{vmatrix} \tilde{\rho}_1 & \tilde{\rho}_2 & \cdots & \cdots & \tilde{\rho}_{M+1} \\ \tilde{\rho}_0 & \ddots & & & \vdots \\ \tilde{\rho}_{-1} & & \ddots & & \vdots \\ \vdots & & & \ddots & \vdots \\ \tilde{\rho}_{1-M} & \cdots & \cdots & \cdots & \tilde{\rho}_1 \end{vmatrix} = 0. \quad (14)$$

Coefficients higher than $M + 1$ can be calculated by repeating this process. Evaluated distribution $D(\theta)$ is nonnegative because

$$\begin{aligned} D(\theta) &= \frac{1}{2\pi} \sum_{m=-M}^M \tilde{\rho}_m e^{jm\theta} \\ &= \frac{1}{2\pi} \sum_{m=-M}^M \left(\lim_{I \rightarrow \infty} \frac{1}{2I+1} \sum_{i=-I}^I f_i f_{i-m}^* \right) e^{jm\theta} \\ &= \frac{1}{2\pi} \lim_{I \rightarrow \infty} \frac{1}{2I+1} \sum_{i=-I}^I f_i e^{ji\theta} \sum_{m=-M}^M (f_m e^{jm\theta})^* \\ &= \frac{1}{2\pi} \lim_{I \rightarrow \infty} \frac{1}{2I+1} \left| \sum_{i=-I}^I f_i e^{ji\theta} \right|^2 \geq 0 \end{aligned} \quad (15)$$

where we assume $I > M$, $\tilde{\rho}_{M+1} = \tilde{\rho}_{M+2} = \dots = \tilde{\rho}_I = 0$.

Eq.(13) requires that the determinants of any order of Toeplitz matrixes must be nonnegative,

$$\begin{vmatrix} \tilde{\rho}_0 & \tilde{\rho}_1 & \cdots & \cdots & \tilde{\rho}_M \\ \tilde{\rho}_{-1} & \ddots & & & \vdots \\ \tilde{\rho}_{-2} & & \ddots & & \vdots \\ \vdots & & & \ddots & \vdots \\ \tilde{\rho}_{-M} & \cdots & \cdots & \cdots & \tilde{\rho}_1 \end{vmatrix} \geq 0. \quad (16)$$

The program not only extrapolates higher order coefficients but modifies lower order ones to make eq.(16) valid. That insures no serious negative lobe of $D(\theta)$.

This MEM procedure is trying to maximize the information entropy of virtual random variable f_i . There seems to be other ways, for example maximizing the entropy of the variable which has the probability density function of $D(\theta)^2$. But that has not been examined yet.

6 FILTERING

In general calculated Fourier coefficients have some error. Moreover MEM extrapolation tends to stop in lower order than expected because of numerical problem and sometimes extrapolated coefficients do not converge smoothly. So we need filtering to get stable estimation of $D(\theta)$. Instead of filtering in θ domain we multiply a Gaussian shape window $W(m)$ to the absolute values of evaluated Fourier coefficients themselves,

$$|\bar{\rho}_m| = W(m) |\hat{\rho}_m| \quad (17)$$

where

$$W(m) = e^{-\frac{m^2}{2\sigma^2}}. \quad (18)$$

The value of the standard deviation σ is decided to make $D(\theta)$ smooth and not to make peaks too low. The window is selected to have a Gaussian shape because if $D(\theta)$ can be expressed with the power of cosine function, we call it "unimodal distribution" hereafter, the absolute values of Fourier coefficients can be approximated with eq.(18).

In the case of unimodal distribution, filtered coefficients can be interpreted as a extended ones to m direction along the shape of eq.(18)⁶,

$$D(\theta) = \frac{1}{2\pi} \sum_{m=-M}^M \bar{\rho}_m e^{jm\kappa\theta} \quad (19)$$

where

$$\bar{\rho}_m = W(m) \hat{\rho}_m e^{(\kappa-1)\phi_m}. \quad (20)$$

From eqs.(18) and (20) the ratio of extension κ is

$$\kappa^2 = 1 - \frac{m^2}{2\sigma^2 \log|\hat{\rho}_m|} \quad (21)$$

κ should be the same value for any order of m . $D(\theta)$ is assumed to be zero for the range out of the new expansion. This unimodal filter works to make the distribution very smooth and to make it sharp when almost long-crested sea comes. But it can be a too strong filter

when we expect a big main peak and small sub peak(s). We should decide if this filter should be used or not by what we expect.

7 APPLICATION TO THE WAVE FIELD NEAR A REFLECTION WALL

Near a reflection wall wave field is not stationary in space because of the interaction between the incident and reflected waves. That can be a serious problem for experiments in model basins and for field measurements near breakwaters and so on. With a wall-sided reflector of coefficient r , cross spectrum of surface elevation measured at \mathbf{x}_1 and \mathbf{x}_2 is,

$$\begin{aligned} \Phi'(\mathbf{x}_2 - \mathbf{x}_1) = \int D(\theta) \{ & e^{j\mathbf{k}\cdot(\mathbf{x}_2 - \mathbf{x}_1)} + r^2 e^{j\mathbf{k}\cdot(\mathbf{x}_{2r} - \mathbf{x}_{1r})} \\ & + r e^{j\mathbf{k}\cdot(\mathbf{x}_2 - \mathbf{x}_{1r})} + r e^{j\mathbf{k}\cdot(\mathbf{x}_{2r} - \mathbf{x}_1)} \} d\theta \end{aligned} \quad (22)$$

where $\mathbf{x}_{i,r}$ means the mirror image of \mathbf{x}_i for the reflector. The first and second terms come from the incident and reflected waves respectively. The third and fourth terms mean the interaction effect³⁾.

Expressing spacial lags with the angles and the distances of the gauge pairs like

$$\begin{aligned} \mathbf{x}_2 - \mathbf{x}_1 &= R \begin{pmatrix} \cos\alpha \\ \sin\alpha \end{pmatrix} \\ \mathbf{x}_{2r} - \mathbf{x}_{1r} &= R \begin{pmatrix} \cos\alpha \\ -\sin\alpha \end{pmatrix} \\ \mathbf{x}_2 - \mathbf{x}_{1r} &= R' \begin{pmatrix} \cos\alpha' \\ \sin\alpha' \end{pmatrix} \\ \mathbf{x}_{2r} - \mathbf{x}_1 &= R' \begin{pmatrix} \cos\alpha' \\ -\sin\alpha' \end{pmatrix} \end{aligned}$$

(see Fig.2), then eq.(22) leads to

$$\begin{aligned} \Phi'(\mathbf{x}_2 - \mathbf{x}_1) = \sum_{m=-\infty}^{\infty} \{ & J_m(kR) (\tilde{\rho}_m + r^2 \tilde{\rho}_m^*) e^{jm(\alpha + \frac{\pi}{2})} \\ & + r J_m(kR') (\tilde{\rho}_m + \tilde{\rho}_m^*) e^{jm(\alpha' + \frac{\pi}{2})} \}. \end{aligned} \quad (23)$$

Note that this equation is not a Fourier expansion because R' and α' , the distance and the angle between the real and imaginary gauges, are the functions of α as follows,

$$R' = \begin{cases} 2y_0 (1 - 2a \cos \gamma \cos \alpha + a^2 \cos^2 \alpha)^{\frac{1}{2}} & (n_e = 1, 2, \dots) \\ 2y_0 (1 + a \sin \alpha + a^2/4)^{\frac{1}{2}} & (n_e = 0) \end{cases} \quad (24)$$

$$\alpha' = \begin{cases} \frac{\pi}{2} - \tan^{-1} \left(\frac{a \sin \gamma \cos \alpha}{1 - a \cos \gamma \cos \alpha} \right) & (n_e = 1, 2, \dots) \\ \frac{\pi}{2} - \tan^{-1} \left(\frac{a \cos \alpha}{2 + a \sin \alpha} \right) & (n_e = 0) \end{cases} \quad (25)$$

where a is the nondimensionalized radius of the circle A/y_0 , and γ is related to nest number

$$\gamma = \frac{\pi}{N} n_e$$

(see Fig.2). If a is small, i.e. the array is located far from the reflector compared to the radius of the array, R' and α' will be reduced to

$$R' \approx 2y_0 \{1 + a \zeta(\alpha; n_e)\} \quad (26)$$

$$\alpha' \approx \frac{\pi}{2} + a \eta(\alpha; n_e) \quad (27)$$

where

$$\zeta(\alpha; n_e) = \begin{cases} -\cos \gamma \cos \alpha & (n_e = 1, 2, \dots) \\ \frac{\sin \alpha}{2} & (n_e = 0) \end{cases}$$

$$\eta(\alpha; n_e) = \begin{cases} -\frac{\sin \gamma \cos \alpha}{\cos \alpha} & (n_e = 1, 2, \dots) \\ -\frac{\cos \alpha}{2} & (n_e = 0). \end{cases}$$

Substituting eq.(23) to eq.(5) and taking an average with Φ'^* just like eq.(10) without paying any attention to the interaction terms we get

$$\hat{\rho}_m = \tilde{\rho}_m + r^2 \tilde{\rho}_m^* + \frac{r}{J_m(kR)} \frac{1}{2\pi} \sum_{l=-\infty}^{\infty} (\tilde{\rho}_{m+2l} + \tilde{\rho}_{m+2l}^*) (-1)^l I_{m+2l,m} \quad (28)$$

where

$$I_{l,m} = \int J_l(kR') \cos(l\alpha') e^{-jm\alpha} d\alpha.$$

So even if we have so many gauges on the circle the evaluated coefficients by CAM will be contaminated by the real parts of $\tilde{\rho}_{m+2l}$'s of the incident wave.

It is not so easy to estimate the behavior of $\hat{\rho}_m$ from eq.(28). So let us assume that $kR' \gg 1$ and $a \ll 1$, i.e. the array is located far from the wall compared to the

wave length and the radius. Using the asymptotic expression of the Bessel function and dropping unimportant terms,

$$\begin{aligned}
 I_{m+2l,m} &= \int J_{m+2l}(kR') \cos\{(m+2l)\alpha'\} e^{-jm\alpha} d\alpha \\
 &\approx \sqrt{\frac{1}{\pi ky_0}} \int \cos\left(2kA\zeta + \beta - \frac{\pi}{2}m\right) \\
 &\quad \cos\left\{(m+2l)a\eta + \frac{\pi}{2}m\right\} e^{-jm\alpha} d\alpha
 \end{aligned} \tag{29}$$

where

$$\beta = 2ky_0 - \frac{\pi}{4}$$

or exchanging the summation and the integration,

$$\begin{aligned}
 \hat{\rho}_m &\approx \tilde{\rho}_m + r^2 \tilde{\rho}_m^* + \frac{r}{J_m(kR)} \sqrt{\frac{1}{\pi ky_0}} \\
 &\quad \cdot \frac{1}{2\pi} \int d\alpha \begin{cases} T_e(\alpha) \cos(2kA\zeta + \beta) e^{-jm\alpha} & (m : \text{even}) \\ -T_s(\alpha) \sin(2kA\zeta + \beta) e^{-jm\alpha} & (m : \text{odd}) \end{cases}
 \end{aligned} \tag{30}$$

where

$$\left. \begin{matrix} T_e(\alpha) \\ T_s(\alpha) \end{matrix} \right\} = \sum_{l=-\infty}^{\infty} (\tilde{\rho}_{m+2l} + \tilde{\rho}_{m+2l}^*) (-1)^l \begin{cases} \cos\{(m+2l)a\eta\} \\ \sin\{(m+2l)a\eta\} \end{cases}$$

From eqs.(28), (29) and (30) we can know some properties of $\hat{\rho}_m$ as follows.

1. Approximately the interaction effect is proportional to $1/\sqrt{ky_0}$.
2. Even number coefficients are easier to be contaminated than odd number ones, because terms of order $\pm(m+2l)$ in $T(\alpha)$ tend to cancel each other by the work of $(-1)^l$ for odd orders.
3. Usually the nest which has the biggest number includes the least interaction effect because ζ , which is proportional to $\cos \gamma$, should be very small (see eq.(26)). We should use the information of this nest as long as $|J_m(kR)|$ is not so small.
4. Too large array leads to bad estimates because of large kA value in eq.(30). On the other hand a small array makes the absolute value of $J_m(kR)$ in the denominator too small. The radius of the same order as the wave length should be recommended.
5. When the incident wave comes almost parallel to the wall the interaction effect will be small because real parts of all $\tilde{\rho}_{m+2l}$'s decay smoothly and those are expected to cancel each other.

6. On the other hand when the incident wave comes with the right angle to the wall we will have serious interaction effect because $\tilde{\rho}_m$'s are proportional to j^m , which means all $\tilde{\rho}_{m+2l}(-1)^l$'s have the same signs. But if m is an odd number we can have an exact estimate because $\tilde{\rho}_{m+2l}$'s have no real parts.
7. As long as $D(\theta)$ has broad and smooth shape, i.e. higher order coefficients are negligible, the interaction term is not so sensitive to the parameter a .

8 SOME SIMULATION RESULTS

Simulations are carried out for $\cos^{2S}\theta$ distributions and superpositions of them. All the results in this report are of cross spectra without noise. The radius of the circular array is 1 meter and 8 wave gauges are used ($N=7$) for all cases. So the maximum order of Fourier coefficients is 13. MEM extrapolation is only used when calculated higher order coefficients are not reliable or when negative lobe(s) cannot be removed by filtering.

Fig.3 shows the results of unimodal distributions using the unimodal filter. In the broadest case the peak is a little lower than the theory because of the filter, but the results are almost satisfactory. When narrow and broad distributions are superimposed like Fig.4 the peak value gets lower because unimodal filter is not used.

The resolution is studied in Fig.5. Two peaks of 25 degrees apart (Fig.5(d)) cannot be distinguished because the resolution of the maximum order, 13, is 27.7 degrees.

Fig.6 is the demonstrations of the MEM extrapolation. In both examples the maximum order of Fourier coefficients before MEM process is 6. Two peaks are clearly separated after MEM because the maximum orders became 19 (Fig.6(a)) and 9 (Fig.6(b)). But in (a) the distribution shapes are a little distorted, and in (b) extrapolation stops at order 9 by a numerical problem. Moreover the resultant directional distributions sometimes have serious fluctuation because extrapolated higher order coefficients do not converge smoothly. There seems to be a room for improvement in MEM extrapolation process.

Calculations on wave fields with a wall reflector of the coefficients $r = 1$ and $r = 0.3$ are shown in Figs.7 and 8 respectively. When $y_0/A \geq 10$ the estimated directional distribution can be almost expressed as the superposition of the incident and reflected waves. But when the array gets closer to the wall we can see not only spurious lobes but also distorted main peaks caused by the standing wave effect. According to another simulation result the reflection wall of the ratio of 0.1 causes no serious fluctuation. So the ability of usual wave absorbers seems to be high enough to get reasonable experimental result, but attention should be paid on the other no-absorbing walls.

The effect of the mean direction of incident wave is also studied in Fig.9. When it is 90 degrees the interaction effect is serious as discussed in the previous section. It is interesting to see that the distribution is the periodic function of π . The reason is all odd

number of coefficients are zero, which is mentioned in item 6. In other directions no serious interaction effect can be seen.

9 CONCLUDING REMARKS

Circular Array Method (CAM) is an unique array-dependent method introduced by C.T.Stansberg⁶⁾ and improved by the author. The Fourier coefficients of directional distribution function calculated by CAM should be more stable than conventional methods as mentioned in section 4.

CAM is basically a linear and simple calculation, so it is easier than other (statistical) methods to estimate the reliability of the result and to find the reason when we get an unexpected distribution. For example if $\hat{\rho}_m$'s in eq.(12) of all nests do not agree well when $J_{m+2lN}(kR)$'s are negligible small, that means cross spectra themselves include significant noise, but if those Fourier coefficients agree well that means the calculated coefficients $\hat{\rho}_m$'s are reliable even if it the directional distribution is not the expected one.

For unimodal wave the resolution is satisfactory using a skillful filter without any extrapolation. But for complicated distributions we should depend on statistical process like MEM, which has some room for future improvement.

When a reflection wall exists the result will be contaminated by the interaction between the incident and reflected waves like other methods. The behavior of it was discussed theoretically. But in practice it is common to take an average with neighboring frequencies, which might cancel some interaction effects if the degree of freedom is large enough. This problem should also be studied further.

10 ACKNOWLEDGEMENTS

I have a regard for the research work of C.T.Stansberg (MARINTEK) on the directional sea problem, and am grateful to him for his advice and encouragement when I was staying in Norwegian Institute of Technology, Trondheim, Norway from 1988 to 1989.

REFERENCES

1. O.H.Oakley and J.B.Loizow : Directional Spectrum Measurement by Small Arrays, OTC2745, (1977)
2. N.Hashimoto and K.Kobune : Estimation of Directional Spectra from the Maximum Entropy Principle, Report of the Port and Harbour Research Institute, Vol.24, No.3, (1985)
3. N.Hashimoto and K.Kobune : Estimation of Directional Spectra from a Bayesian Approach in Incident and Reflected Wave Field, Report of the Port and Harbour Research Institute, Vol.26, No.4, (1987)
4. L.E.Borgman : Directional Spectra Models for Design Use, OTC1069, (1969)
5. T.J.Ulrych and T.N.Bishop : Maximum Entropy Spectral Analysis and Autoregressive Decomposition, Review of Geophysics and Space Physics, Vol.13, No.1, (1975)
6. C.T.Stansberg : Numerical Study on Methods for Directional Spectrum Simulation and Estimation, Symposium on Description and Modeling of Directional Seas, (1984)
7. C.T.Stansberg : Statistical Properties of Directional Sea Measurements, Journal of Offshore Mechanics and Arctic Engineering, (1987)
8. C.T.Stansberg and S.Ishida : Directional Spectrum Estimation by Means of a Circular Wave Gauge Array, Proc. of 23rd Congress of IAHR, (1989)

Abstract

For estimating the directional spectrum of short-crested seas Circular Array Method (CAM) is proposed. CAM is an array-dependent method, distributing an odd number of wave gauges on a circle and one on the center of the circle. Through this array arrangement the Fourier coefficients of the directional distribution function can be evaluated by a simple calculation, inverse Fourier transformation of cross spectrum. But for higher orders MEM extrapolation is used.

Fourier coefficients are calculated directly and distinctly with simple equation, so it is easier than other methods (e.g. MLM) to estimate the reliability of the result and to find the reason when we get an unexpected directional distribution. For a single-peak distribution the resolution of CAM is satisfactory with a skillful filter, but for complicated distribution there is a room for improvement of MEM extrapolation process.

Standing wave effect caused by a reflection wall can be a serious problem for experiments in model basins and for field measurements. Application of CAM to those wave fields was studied qualitatively and quantitatively. The behavior of the interaction term was discussed relating to the distance of the array from the wall, the array size, the incident angle to the wall and so on. These discussions were confirmed by simulations.

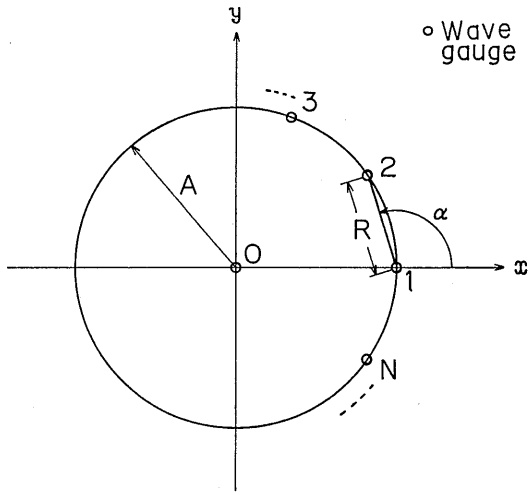


Fig. 1 Geometry of Circular Array

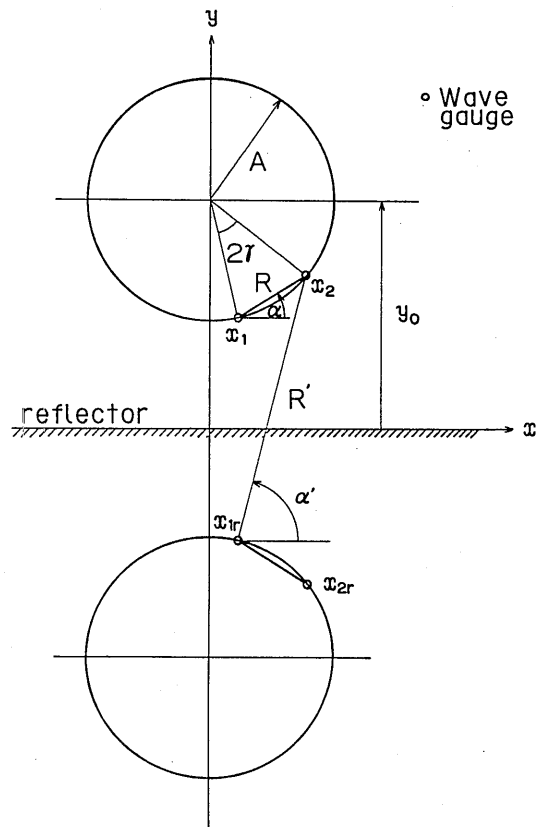
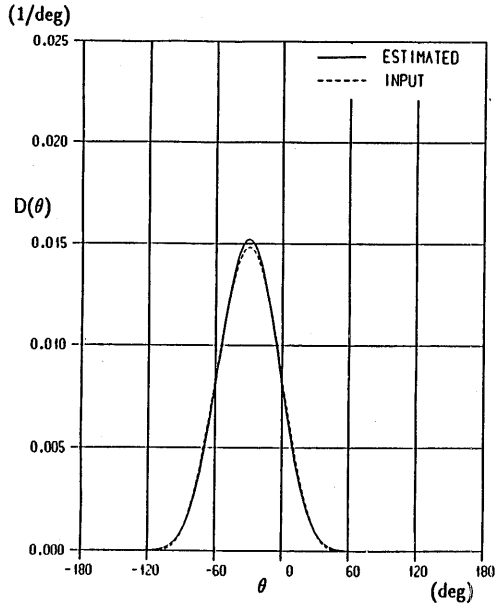
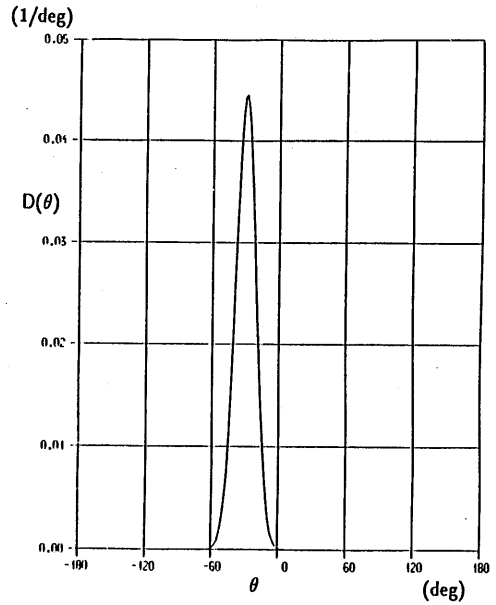


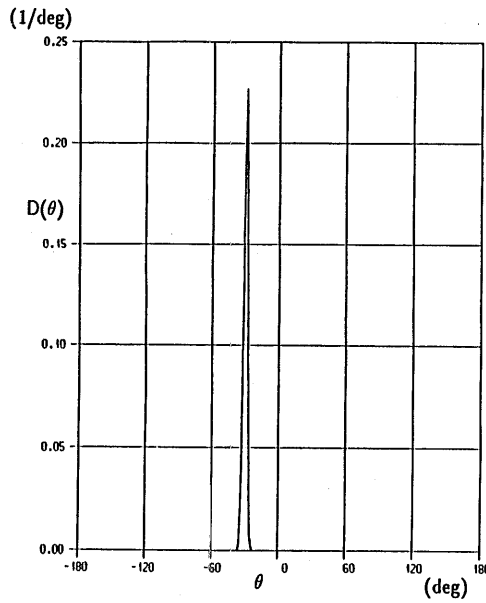
Fig. 2 Mirror Image of Circular Array with a Reflection Wall



(a) $S = 2$



(b) $S = 20$



(c) $S = 500$

Fig. 3 Simulation of Unimodal Distribution,
 $D(\theta) \propto \cos^{2S}(\theta + \frac{\pi}{6})$, $f = 0.96$ Hz

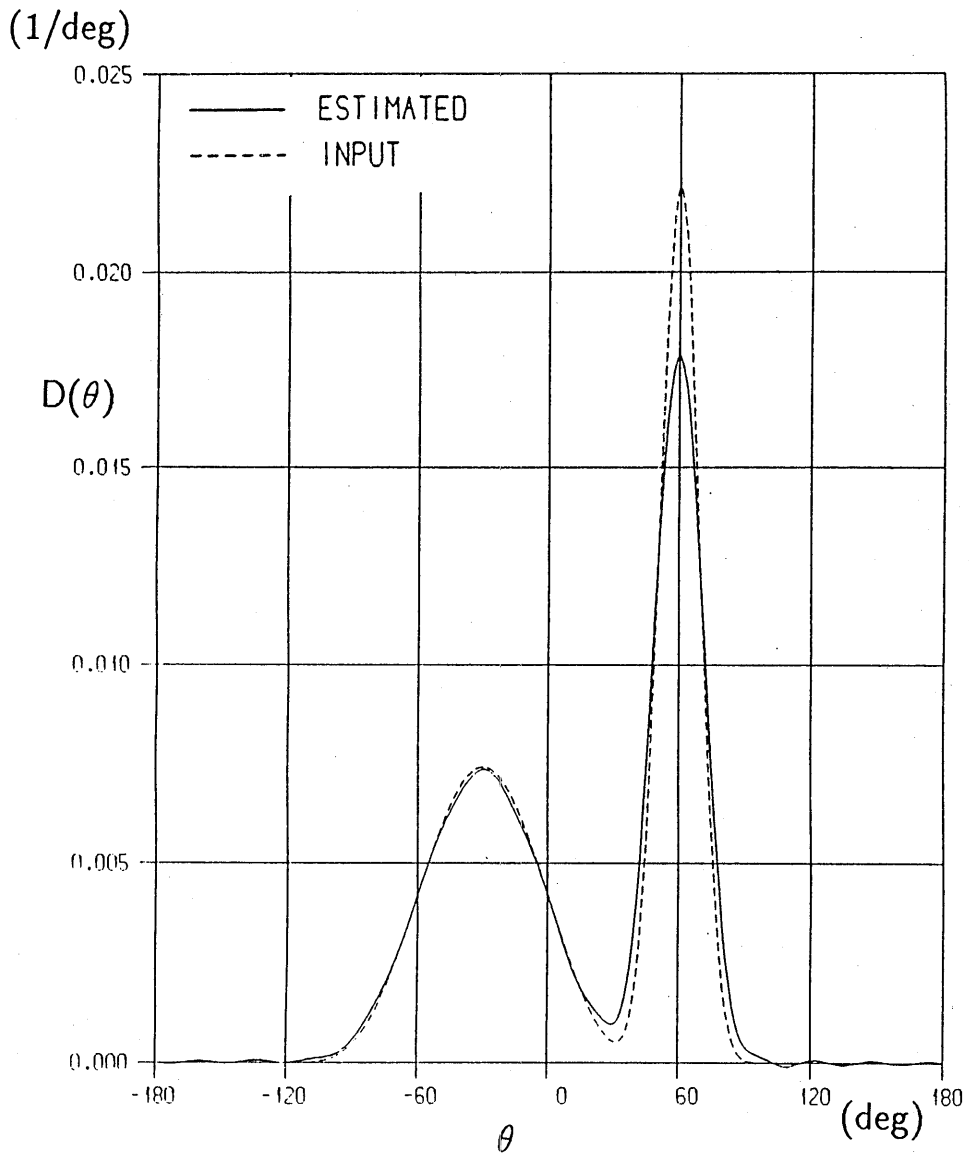
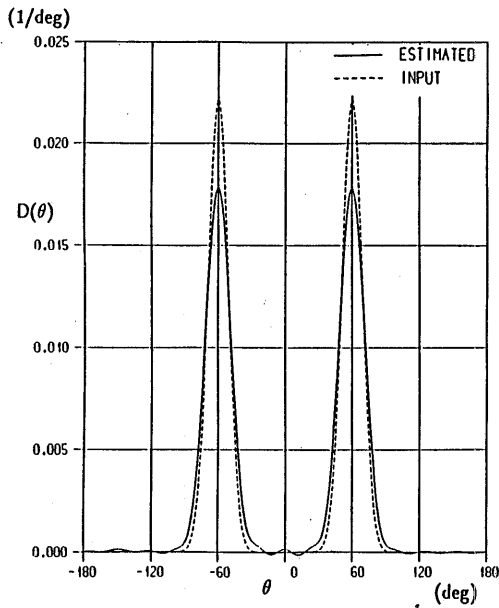


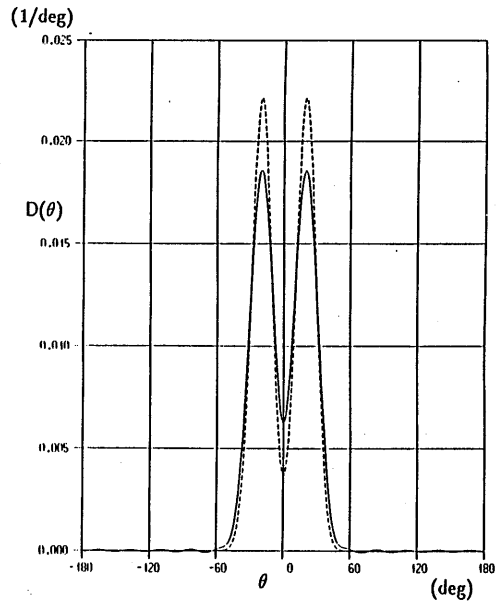
Fig. 4

Simulation of Bimodal Distribution,

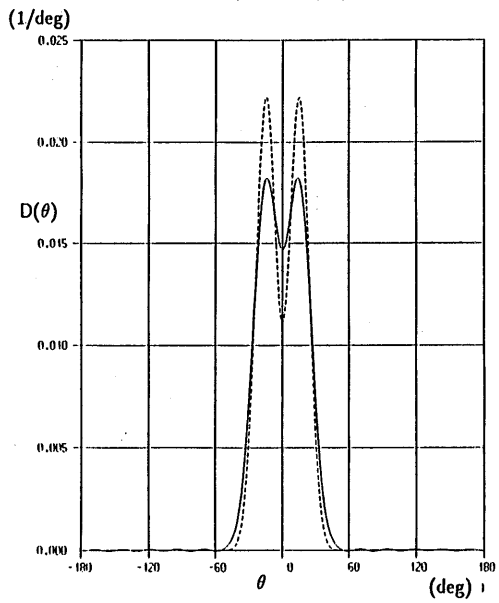
$$D(\theta) \propto \cos^4\left(\theta + \frac{\pi}{6}\right) + 3 \cos^{4^{\circ}}\left(\theta - \frac{\pi}{3}\right), \quad f = 0.96 \text{ Hz}$$



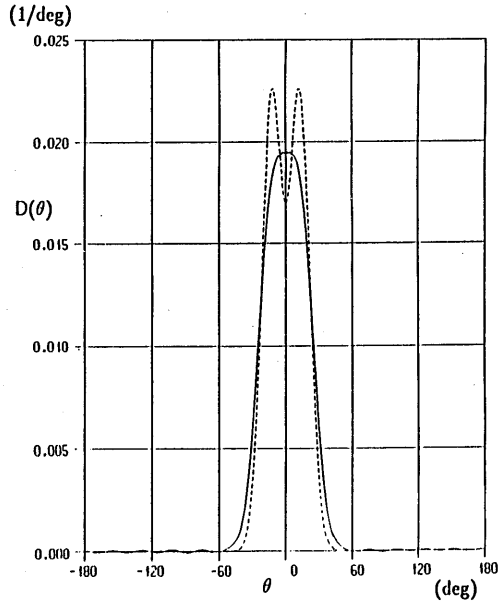
(a) $\theta_0 = \frac{\pi}{3}$



(b) $\theta_0 = \frac{\pi}{9}$



(c) $\theta_0 = \frac{\pi}{12}$



(d) $\theta_0 = \frac{\pi}{14.4}$

Fig. 5 Resolution of CAM,
 $D(\theta) \propto \cos^{4\theta}(\theta - \theta_0) + \cos^{4\theta}(\theta + \theta_0)$, $f = 0.96$ Hz

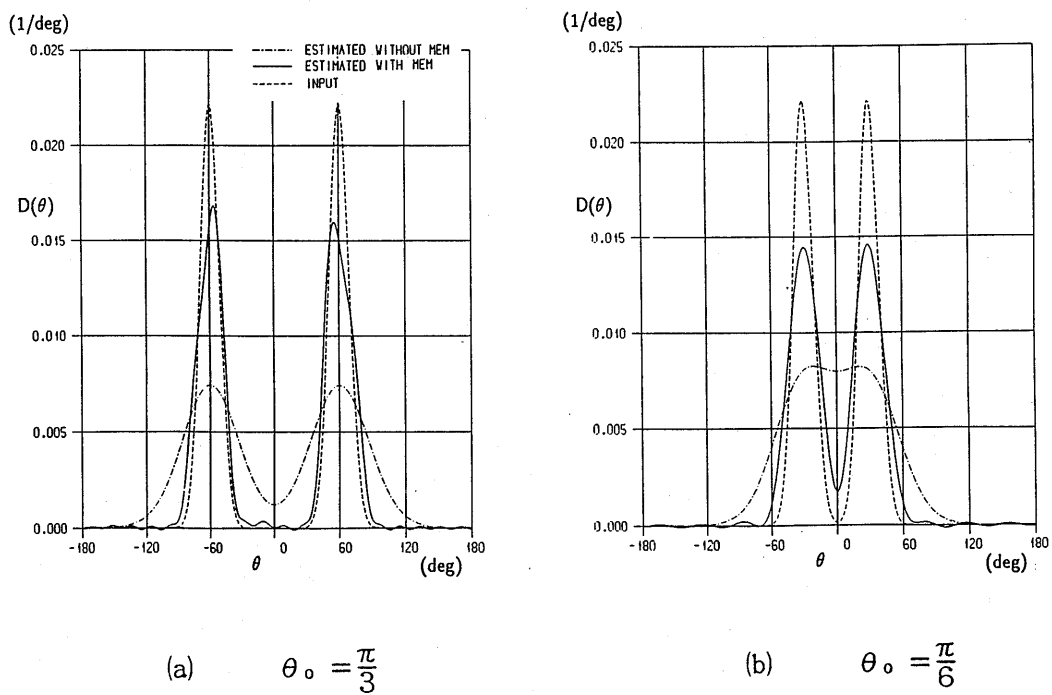
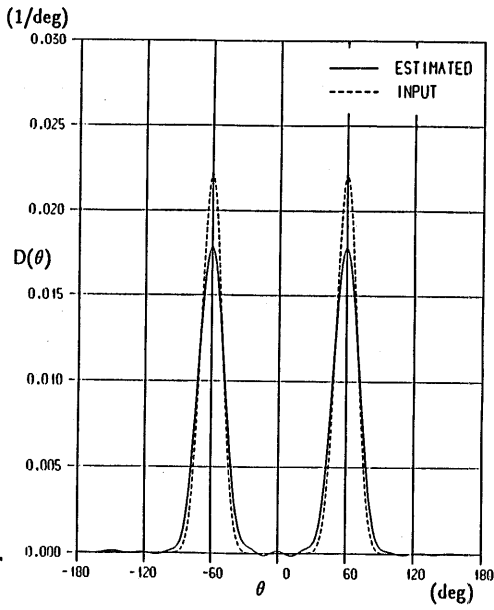
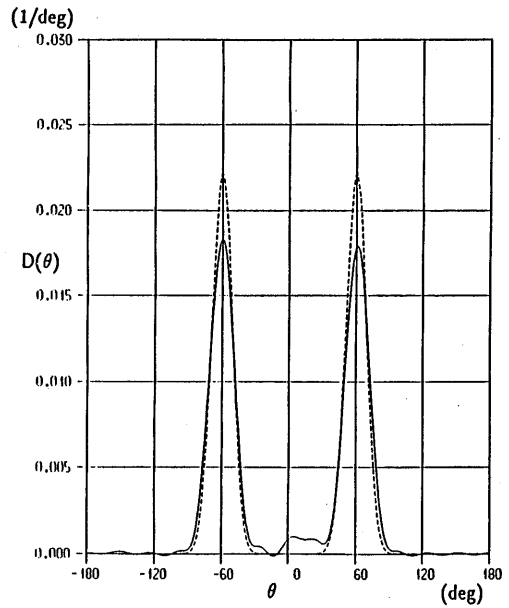


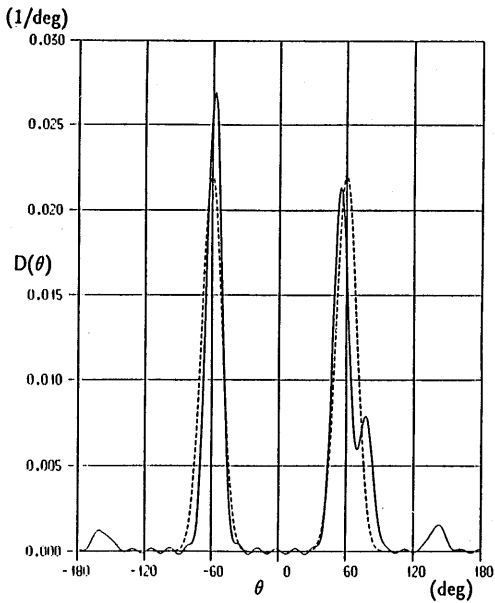
Fig. 6 Behavior of MEM Extrapolation,
 $D(\theta) \propto \cos^{4\theta}(\theta - \theta_0) + \cos^{4\theta}(\theta + \theta_0)$, $f = 0.33$ Hz



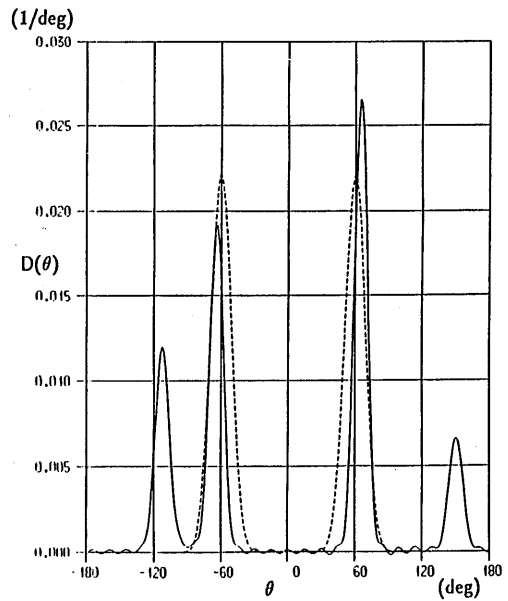
(a) $y_0 / A = \infty$



(b) $y_0 / A = 10$



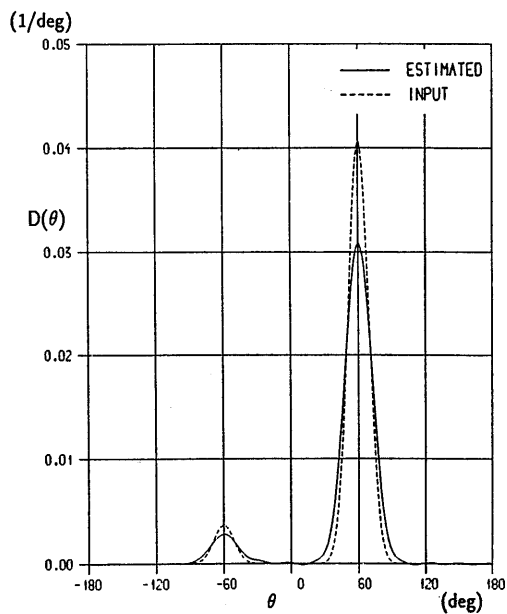
(c) $y_0 / A = 5$



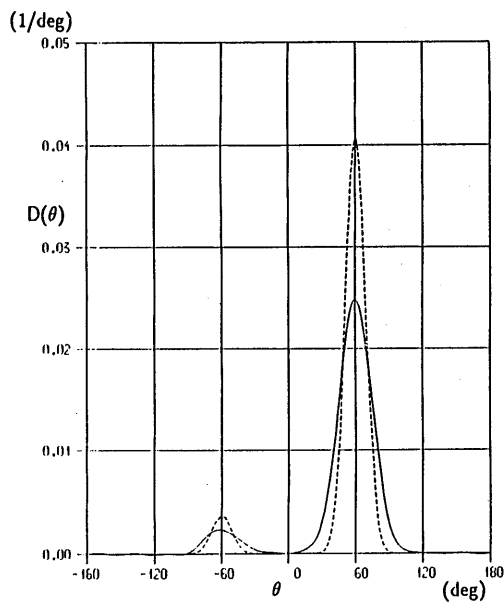
(d) $y_0 / A = 2.5$

Fig. 7 Directional Distribution with a Reflection Wall,

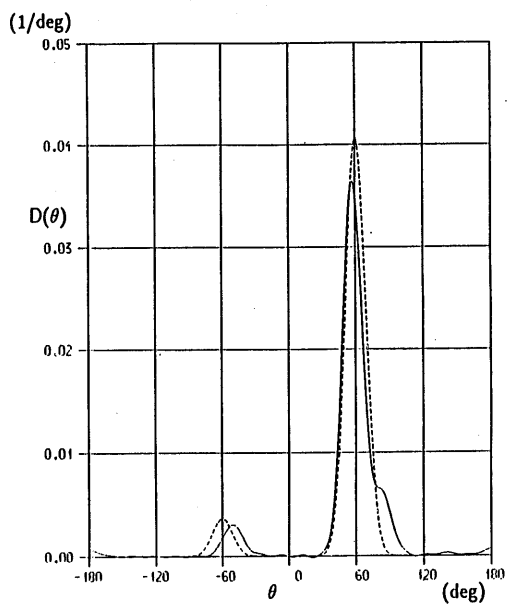
$$D(\theta) \propto \cos^4\left(\theta - \frac{\pi}{3}\right), \quad r=1.0, \quad f = 0.96 \text{ Hz}$$



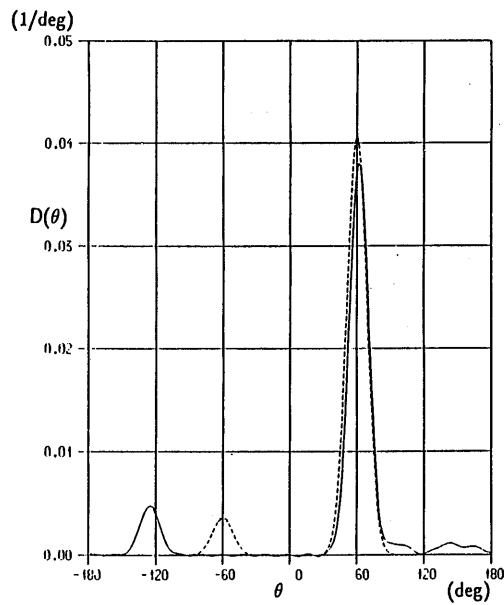
(a) $y_0 / A = \infty$



(b) $y_0 / A = 10$

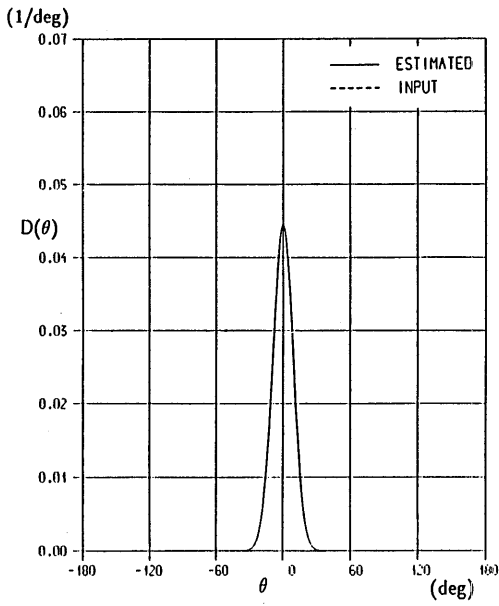


(c) $y_0 / A = 5$

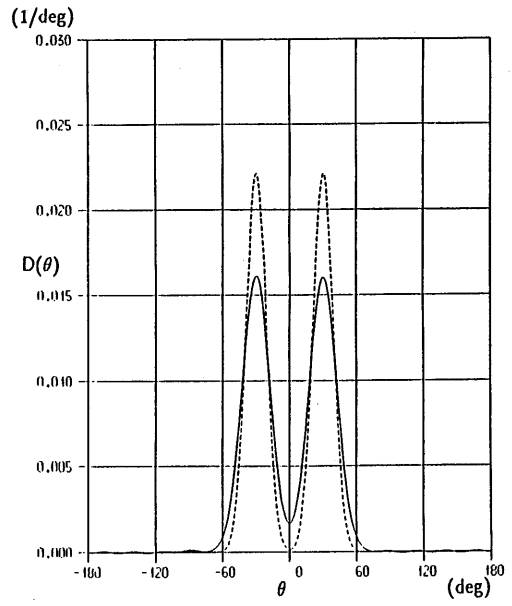


(d) $y_0 / A = 2.5$

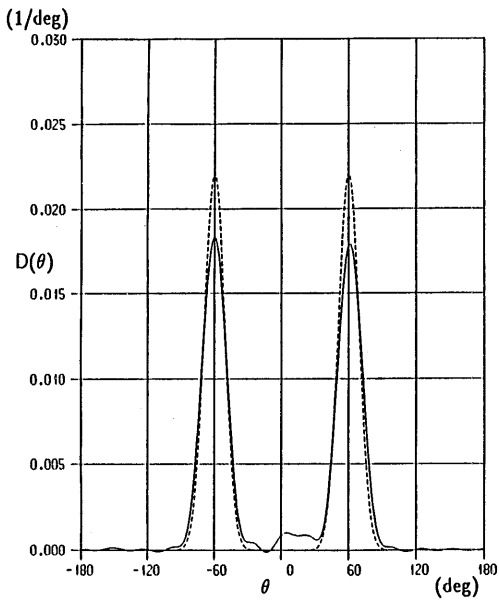
Fig. 8 Directional Distribution with a Reflection Wall,
 $D(\theta) \propto \cos^4 \left(\theta - \frac{\pi}{3} \right)$, $r = 0.3$, $f = 0.96$ Hz



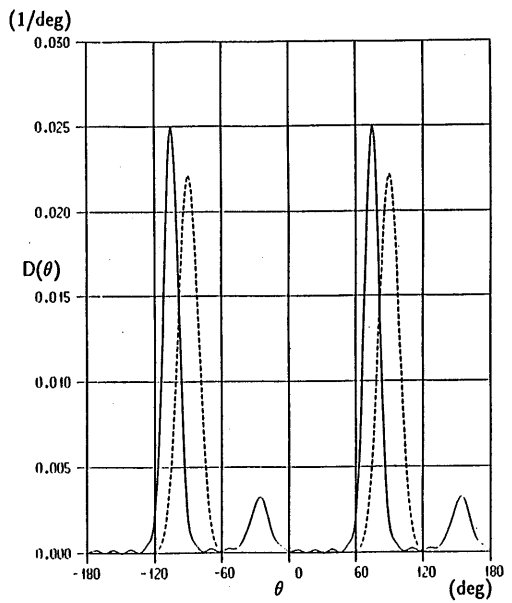
(a) $\theta_0 = 0$



(b) $\theta_0 = \frac{\pi}{6}$



(c) $\theta_0 = \frac{\pi}{3}$



(d) $\theta_0 = \frac{\pi}{2}$

Fig. 9

Directional Distribution with a Reflection Wall,

$$D(\theta) \propto \cos^4(\theta - \theta_0), \quad r=1.0, \quad y_0/A=1.0, \quad f=0.96 \text{ Hz}$$